Table 3 Clinical features of codon 129 heterozygosity of methionine/valine between V180I and sCJD-MV

	V180I-MV n=45	sCJD-MV n=7	p Value
Type 1 or 2		5 type 2; 2 NA	
Male/female	20/25	3/4	1
Codon 219	44 EE; 1 EK	7 EE	
Age at onset (years)*	76.7±7.6 (78, 57–92, n=43)	62.0±7.0 (62, 51–73, n=7)	<0.001
Period from onset to death (months)*	27.8±16.3 (25, 7–64, n=23)	26.2±12.9 (21, 12–43, n=6)	0.98
Myoclonus†	21/43 (48.8%)	5/7 (71.4%)	0.42
Period from onset to myoclonus (months)*	9.2±7.2 (7, 2–30, n=18)	8.5±4.7 (7.5, 4–15, n=4)	0.86
Cognitive impairment†	43/44 (97.7%)	7/7 (100%)	1
Period from onset to cognitive impairment (months)*‡	0.6±1.4 (0, 0–5, n=38)	3.0±4.5 (0, 0–10, n=5)	0.26
Pyramidal signs†	14/42 (33.3%)	2/6 (33.3%)	1
Period from onset to pyramidal sign (months)*	5.2±4.2 (5, 0–14, n=11)	12 (n=1)	
Extrapyramidal signs†	23/40 (57.5%)	5/6 (83.3%)	0.23
Period from onset to extrapyramidal signs (months)*	3.8±4.5 (2, 0–16, n=18)	5.5±6.6 (4, 0–15, n=4)	0.58
Cerebellar dysfunction†	12/38 (31.6%)	6/6 (100%)	0.003
Period from onset to cerebellar dysfunction (months)*	3.4±4.1 (3, 0–12, n=8)	5.8±5.4 (4, 0–14, n=5)	0.50
Visual disturbance†	1/34 (2.9%)	1/5 (20%)	0.24
Period from onset to visual disturbance (months)*	(n=0)	(n=0)	
Psychiatric symptoms†	16/38 (42.1%)	3/7 (42.9%)	1
Period from onset to psychiatric symptoms (months)*	2.0±2.6 (0, 0–7, n=13)	4.5±2.1 (5, 3–6, n=2)	0.24
Akinetic mutism†	30/44 (68.2%)	3/7 (42.9%)	0.23
Period from onset to akinetic mutism (months)*	13.2±10.9 (9, 0–49, n=23)	12.5±5.0 (13, 9–16, n=2)	
PSWCs on EEG†	5/39 (12.8%)	2/6 (33.3%)	0.23
Hyperintensities on MRI	44/44 (100%)	7/7 (100%)	1
Positive rate of 14-3-3 protein in CSF†	11/18 (61.1%)	NA	
Positive rate of t-τ protein in CSF†	12/18 (66.7%)	NA	
Amount of t-τ protein in CSF (pg/mL)*	2025±1441 (1689, 170.0–6430.0, n=18)	NA	
Positive rate of PrP^{Sc} in CSF†	7/18 (38.9%)	NA	

Codon 219 is presented with total cases of that polymorphism type. EE and EK mean glutamic acid and glycine homozygous, respectively.
NA *means data not available.*
Medians are compared using the two-tailed Mann-Whitney U test for age of onset, the period from disease onset to death or the appearance of each symptom and sign and the CSF biomarker level. Frequencies of positive cases are compared using the two-tailed Fisher's exact test.
*Age at onset, period of time from disease onset to death or the appearance of each symptom and sign and CSF biomarker level are presented as mean±SD (median, range, cases).
†Frequencies of positive cases are presented as positive cases/total cases (percentage).
‡These were zero-inflated.
CSF, cerebrospinal fluid; PSWCs, periodic sharp wave complexes; sCJD, sporadic Creutzfeldt-Jakob disease; t-τ, total τ.

The average age of onset in V180I-MM and V180I-MV was about 10 years older than those of sCJD-MM1 and sCJD-MM2, and MV2, respectively. The period from disease onset to death was longer in V180I-MM than in sCJD-MM1, as previously reported,[4] but was almost the same as in sCJD-MM2 (table 2). Among the 16 total autopsied patients with V180I in this cohort, few patients had additional neuropathological alterations such as Alzheimer's disease.[6 7] There was no difference between definite and probable or possible cases with V180I mutation. The periods from onset to the occurrence of myoclonus, cerebellar dysfunction, visual disturbance and akinetic mutism in V180I-MM were significantly longer than those in sCJD-MM1. However, except for visual disturbance, the length of onset to the occurrence of all other signs was shorter than those in sCJD-MM2 (table 2). As for the clinical features of 129MV, there was no significant difference between V180I-MV and sCJD-MV, except for age of onset (table 3).

The analysis of the probability of occurrence of neurological symptoms and signs similarly demonstrated reduced severity in patients with V180I-MM compared to those with sCJD-MM1. While 88.1% of patients with sCJD-MM1 developed myoclonus, only 35.4% of patients with V180I developed myoclonus. Pyramidal signs, cerebellar dysfunction, visual disturbance and akinetic mutism were also less frequent in patients with V180I-MM1 than in patients with sCJD-MM1. However, as previously reported,[9] cerebellar and visual systems were not completely spared in patients with V180I.

EEG and MRI findings

PSWCs were observed in only 7.3% of patients with V180I-MM, but in over 90% of patients with sCJD-MM1 (table 2). MRI revealed hyperintensities with a similar positive rate in V180I-MM and sCJD-MM1, but was observed less frequently in patients with sCJD-MM2. The

Table 4 Effects of the codon 129 polymorphism on the clinical features of V180I

	129MM n=139	129MV n=45	p Value
Male/female	58/81	20/25	0.862
Age at onset (years)*	77.3±6.8 (78, 44–93, n=139)	76.7±7.6 (78, 57–92, n=45)	0.701
Period from onset to death (months)*	23.1±15.1 (19, 5–70, n=75)	27.8±16.3 (25, 7–64, n=23)	0.159
Myoclonus†	46/130 (35.4%)	21/43 (48.8%)	0.149
Period from onset to myoclonus (months)*	6.4±6.1 (5, 0–36, n=38)	9.2±7.2 (7, 2–30, n=18)	0.154
Cognitive impairment†	138/138 (100.0%)	43/44 (97.7%)	0.242
Period from onset to cognitive impairment (months)*	0.5±1.4 (0, 0–7, n=121)	0.6±1.4 (0, 0–5, n=38)	0.456
Pyramidal signs†	66/132 (50.0%)	14/42 (33.3%)	0.075
Period from onset to pyramidal signs (months)*	3.9±5.8 (3, 0–36, n=58)	5.2±4.2 (5, 0–14, n=11)	0.136
Extrapyramidal signs†	71/133 (53.4%)	23/40 (57.5%)	0.719
Period from onset to extrapyramidal signs (months)*	3.8±3.5 (3, 0–19, n=58)	3.8±4.5 (2, 0–16, n=18)	0.460
Cerebellar dysfunction†	40/119 (33.6%)	12/38 (31.6%)	1.000
Period from onset to cerebellar dysfunction (months)*	2.9±2.7 (3, 0–9, n=33)	3.4±4.1 (3, 0–12, n=8)	0.973
Visual disturbance†	10/109 (9.2%)	1/34 (2.9%)	0.460
Period from onset to visual disturbance (months)*	2.2±1.5 (2, 0–4, n=10)	(n=0)	NA
Psychiatric symptoms†	68/130 (52.3%)	16/38 (42.1%)	0.357
Period from onset to psychiatric symptoms (months)*	1.6±3.0 (0, 0–19, n=62)	2.0±2.6 (0, 0–7, n=13)	0.576
Akinetic mutism†	74/137 (54.0%)	30/44 (68.2%)	0.116
Period from onset to akinetic mutism (months)*	9.8±6.6 (8, 1–27, n=64)	13.2±10.9 (9, 0–49, n=23)	0.190
PSWCs on EEG†	10/131 (7.6%)	5/39 (12.8%)	0.339
Hyperintensities on MRI†	135/136 (99.3%)	44/44 (100.0%)	1.000
Positive rate of 14-3-3 protein in CSF†	46/53 (86.8%)	11/18 (61.1%)	0.035
Positive rate of t-τ protein in CSF†	48/53 (90.6%)	12/18 (66.7%)	0.014
Amount of t-τ protein in CSF (pg/mL)*	2965±1712 (2400, 146.0–9940.0, n=53)	2025±1441 (1689, 170.0–6430.0, n=18)	0.022
Positive rate of PrP^{Sc} in CSF†	36/53 (67.9%)	7/18 (38.9%)	0.049

*Age of onset, period from disease onset to death or the appearance of each symptom and sign and CSF biomarker level are presented as mean±SD (median, range, case number).
†Frequencies of positive cases are presented as positive cases/total cases (percentage).
Medians are compared using the two-tailed Mann-Whitney U test for age of onset, the period from disease onset to death or the appearance of each symptom and sign and the CSF biomarker level. Frequencies of positive cases are compared using the two-tailed Fisher's exact test.
CSF, cerebrospinal fluid; PSWCs, periodic sharp wave complexes; t-τ, total τ.

pattern of hyperintensities in patients with V180I was uniquely distributed in the cerebral cortex.

Effect of *PRNP* polymorphism on clinical symptoms and signs of V180I

We also analysed the effect of the codon 129 polymorphism on the clinical symptoms of patients with V180I (table 4).

In a total of 184 patients with V180I, 139 patients (75.5%) were 129MM, while the remaining 45 (24.5%) were 129MV. We detected only three patients with the V180I mutation on the same allele as valine. In this case, the clinical features were no different from those with the mutation on the same allele as methionine. We also analysed the codon 219 polymorphism in 179 patients with V180I and 54 patients with sCJD-MM1, all of whom showed glutamic acid homozygosity (table 2). When analysing the influence of the codon 129 polymorphism on clinical symptoms and signs in patients with V180I, no symptoms or signs, in terms of the occurrence rate and the speed to develop them after disease onset, were affected by codon 129MV.

CSF biomarkers

Positive tests of the CSF 14-3-3 protein and t-τ proteins in patients with V180I-MM were similar to those of patients with sCJD-MM1 (table 2). However, the median value of t-τ proteins in the CSF of patients with V180I-MM was significantly lower than that of patients with sCJD-MM1. In patients with V180I-MM, we found fewer positive tests for PrP^{Sc} in the CSF than in patients with sCJD-MM1. Patients with V180I-MV, in particular, showed significantly fewer positive tests for 14-3-3, t-τ protein and PrP^{Sc} in the CSF, as well as in the amount of CSF t-τ (p=0.034, 0.023, 0.001 and <0.001, respectively; multiple comparison using Fisher's exact and Kruskal-Wallis tests).

Effect of age

In order to exclude whether any variables were age dependent, we compared some laboratory and CSF findings in patients with V180I and with sCJD older than 75 years (table 5). We found that positive rates of PrP^{Sc} were comparable, although whether the greater percentage of older patients with PrP^{Sc} is age dependent or due to the small sample size is currently unclear.

Table 5 Laboratory and CSF findings of gPrD-V180I compared to sCJD older than 75 years

	V180I n=186	sCJD (>75 years) n=11	p Value
Male/female	78/108	25/34	1.00
Age at onset (years)*	77.2±6.9 (78, 44–93)	80.9±4.2 (80, 76–89)	0.056
PSWCs on EEG†	16/172 (9.3%)	10/11 (90.9%)	<0.001
Positive rate of 14-3-3 protein in CSF†	57/71 (80.2%)	7/8 (87.5%)	1.00
Positive rate of t-τ protein in CSF†	61/71 (85.9%)	6/8 (75.0%)	0.60
Amount of t-τ protein in CSF (pg/mL)*	2727±1688 (2400, 146.0–9940.0, n=71)	6569.8±4270.3 (8995.0, 150.0–10290.0, n=8)	0.035
Positive rate of PrP^{Sc} in CSF†	44/71 (62.0%)	7/8 (87.5%)	0.246

Medians are compared using the two-tailed Mann-Whitney U test for age at onset, the period from disease onset to death or the appearance of each symptom and sign and the CSF biomarker level. Frequencies of positive cases are compared using the two-tailed Fisher's exact test.
*Age at onset and the appearance of CSF biomarker level are presented with mean±SD (median, range, case number).
†Frequencies of positive cases are presented with positive case number/total case number (percentage).
CSF, cerebrospinal fluid; gPrD, genetic form of prion disease; PSWCs, periodic sharp wave complexes; sCJD, sporadic Creutzfeldt-Jakob disease; t-τ, total τ.

DISCUSSION

With a very rare incidence in Europe,[3] the V180I mutation was geoepidemiologically discovered mainly in Japan, and has turned out to be the most common cause of gPrD in Japan.[5] The reason for this geographical distribution difference is currently unclear, but racial and/or environmental factors are most likely involved.

Of the patients with V180I gPrD, 78 cases were of male patients and 108 cases were female, indicating a possible gender influence on the susceptibility of this mutation in the disease. Similar to other mutations in *PRNP*, women appear more susceptible.[3] Patients with sCJD-MM1 were characterised by fast, severe progression of the disease, and neurological malfunctions resulting from extensive brain lesions appeared in a period of less than 3 months (table 2). However, V180I progressed relatively slowly. Myoclonus, cerebellar signs and visual dysfunctions occurred less frequently and with greater latency in patients with V180I (table 2). PSWCs in the EEG, a frequent finding in patients with sCJD-MM1, were rarely detected in patients with V180I (table 2). While a triad of dementia, myoclonus and PSWCs in the EEG is typical of sCJD, patients with V180I mainly presented with cognitive impairment and a very low rate of myoclonus in the early stages, along with rarely detectable PSWCs. Instead of possible CJD, these cases tended to be misdiagnosed as dementia due to Alzheimer's disease. MRI could facilitate the diagnosis of V180I when a specific pattern of ribbon hyperintensity lesions is detected.[8 13] However, it may still be difficult to distinguish patients with V180I from patients with sCJD-MM1 because hyperintensity was similarly detected in patients with sCJD-MM1, necessitating direct testing of the *PRNP* gene.

Previous reports suggested that there were no visual and cerebellar clinical symptoms in V180I, and neuroimaging of the medial occipital lobes posterior to the parieto-occipital sulcus and the cerebellum revealed that they were not involved until the terminal stage.[9] These data posit V180I as a comparative analogue of sCJD[14] or a cortical form of sCJD with type-2 PrP^{Sc} and methionine homozygosity at codon 129.[15] In our current study of 186 patients with V180I, we found that 34% demonstrated clinical cerebellar dysfunction, and 8.3% presented with visual disturbances (tables 2 and 3). Although no detailed description of the exact manifestations of cerebellar and visual symptoms was recorded, and a subjective bias in identifying the true origins of these symptoms should be taken into consideration, our finding indicates that in order to confirm whether the cerebellum is actually spared in patients with V180I, it is critical to analyse the pathological and immunohistochemical features including PrP^{Sc} deposition and spongiform changes in a topological manner.

The penetrance of V180I was very low. Only 11 out of 186 patients (5.9%) had a family history of dementia, while family member involvement in the case of other gPrD mutations, such as E200K, P102L and P105L, was frequently noted.[3 5] Within the 11 patients with V180I in the current study who had a recorded family history, 3 patients had one family member each diagnosed with CJD. The remaining eight cases had family members of one generation above, or the same generation, who had dementia due to an unknown cause. The low penetrance of V180I, specific clinical features and MRI findings was intriguing, and leads us to speculate whether the V180I mutation is causative for the disease or is actually a disease-associated factor accompanying other protective or toxic factors. The V180I mutation is reported to have significantly higher proportions of overall prion disease (n=881, both $p<0.001$),[4] compared with the genotypes of *PRNP* in the general Japanese population (n=466; isoleucine allele at codon 180 was not detected).[16] These findings indicate that the V180I mutation is not simply a polymorphism, but is indeed disease related.

Different PrP^{Sc} glycotypes might lead to differential distributions of PrP^{Sc} throughout the brain,[17 18] and may account for the disparate affects on brain regions

underlying cerebral cortical symptoms as opposed to cerebellar symptoms, for instance. In this cohort, western blotting of brain homogenates from patients with V180I indicated only weak bands of the monoglycosylated and unglycosylated fragments.[5] In the future, studies should examine the role of factors that influence lesion topology on the disease's clinical expression and progression. We hypothesise that the different pattern of clinical and pathological features with V180I may represent different, but still topologically defined, neuronal loss when compared with sCJD-MM1. Elucidating this mechanism would require systematic pathological, immunochemical and biochemical studies of PrP^{Sc}.

The codon 129 polymorphism in *PRNP* plays an important role in determining the disease phenotype and the type of PrP^{Sc} present in sCJD.[14 19 20] It was also reported that the codon 129 polymorphism affects the phenotype in gPrD.[21–23] In our study, while 75.5% had methionine in the normal allele (MM homozygous), 24.5% had valine in the normal allele (MV heterozygous). We observed that when the codon 129 polymorphism occurred in the allele opposite to the V180I mutation, its influence on the clinical symptoms and signs were similar to the wild type MV polymorphism (table 4). However, the MV polymorphism in codon 129 significantly lowered the positive test rate and amount of CSF biomarkers such as the 14-3-3 protein, τ protein and PrP^{Sc} positivity, suggesting that the codon 129 polymorphism may contribute to the severity and/or speed of neurological degeneration. Moreover, there might be other unknown disease modifying factors that contribute to the clinical features and course of genetic prion disease. In addition, the codon 129 and 219 polymorphisms have been reported to be risk and protective factors, respectively, for sCJD.[24–27] In our study, similar to the study of patients with sCJD-MM1, all patients with V180I tested for the codon 219 polymorphism were glutamic acid homozygous (table 2). This result further suggests that codon 219 heterozygosity would be a protective factor in resisting prion disease onset. Interestingly, the frequency of codon 129 in MV heterozygous patients with the V180I mutation is greater than that in the general Japanese population, creating a discrepancy in the hypothesis that codon 129 homozygosity increases the susceptibility to prion disease.

Although there are several reports describing V180I in terms of its clinical features, imaging characteristics, pathology, immunohistochemistry and biochemistry, most were either case reports or analyses of a small number of cases.[6–8 28–31] To the best of our knowledge, the current study is the first large cohort clinical study of V180I. From this study, we conclude the clinical features of V180I to be as follows: (1) a late age of onset and slow progression; (2) a relatively low occurrence rate, and slow development of symptoms such as myoclonus, cerebellar abnormalities and visual disturbances; (3) a low detectable rate of PSWCs in EEGs, and a high detectable rate of hyperintensity in diffusion-weighted or fluid-attenuated inversion recovery imaging; (4) lower t-τ protein levels in the CSF versus sCJD-MM1 and (5) an extremely low likelihood of a family history of V180I.

Author affiliations
[1]Department of Neurology and Neurological Science, Tokyo Medical and Dental University Graduate School of Medical and Dental Sciences, Tokyo, Japan
[2]Faculty of Medicine, Clinical Research Center, Tokyo Medical and Dental University, Tokyo, Japan
[3]Department of Molecular Microbiology and Immunology, Nagasaki University Graduate School of Biomedical Sciences, Nagasaki, Japan
[4]Department of Neurology, National Hospital Organization Iou Hospital, Kanazawa, Japan
[5]Department of Neurology and Neurobiology of Aging, Kanazawa University Graduate School of Medical Science, Kanazawa, Japan
[6]Department of Public Health, Jichi Medical University, Tochigi, Japan
[7]Division of CJD Science and Technology, Department of Prion Protein Research, Tohoku University Graduate School of Medicine, Miyagi, Japan
[8]Department of Neurology and Neuropathology, Tokyo Metropolitan Geriatric Hospital and Institute of Gerontology, Tokyo, Japan
[9]Department of Neurology, Neurological Institute, Kyushu University Graduate School of Medicine, Fukuoka, Japan

Acknowledgements The authors are grateful to all the members of the Prion Disease Surveillance Committee, Japan, for collecting data and offering advice. They also thank the patients with CJD and their families for providing clinical information about the patients. Our manuscript has been edited by professional native English-speaking editors (http://www.editage.jp).

Contributors TQ drafted the manuscript and analysed the data. NS and M Hizume revised the manuscript, designed the study and analysed the data. NS and MT performed the statistical analysis and obtained funding. RA and KS analysed the CSF samples. M Higuma, IN, TH, SM and AK coordinated the study. TK analysed the prion protein gene and supervised the study. YN collected patient data. MY and HM supervised this study.

Funding The contributions of NS, YN, TK, MY and HM to this study were supported in part by a Health and Labour Sciences Research Grant for Research on Measures for Intractable Diseases (Prion Disease and Slow Virus Infections, the Research Committee on Surveillance and Infection Control of Prion Disease) from the Ministry of Health, Labour and Welfare of the Japanese government.

Competing interests None.

Patient consent Obtained.

Ethics approval Institutional Ethics Committee of Tokyo Medical and Dental University.

Provenance and peer review Not commissioned; externally peer reviewed.

Data sharing statement No additional data are available.

REFERENCES

1. Collinge J. Prion diseases of humans and animals: their causes and molecular basis. *Annu Rev Neurosci* 2001;24:519–50.
2. Ironside JW, Ritchie DL, Head MW. Phenotypic variability in human prion diseases. *Neuropathol Appl Neurobiol* 2005;31:565–79.
3. Kovacs GG, Puopolo M, Ladogana A, *et al.* Genetic prion disease: the EUROCJD experience. *Hum Genet* 2005;118:166–74.
4. Nozaki I, Hamaguchi T, Sanjo N, *et al.* Prospective 10-year surveillance of human prion diseases in Japan. *Brain* 2010;133:3043–57.

5. Higuma M, Sanjo N, Satoh K, *et al.* Relationships between clinicopathological features and cerebrospinal fluid biomarkers in Japanese patients with genetic prion diseases. *PLoS ONE* 2013;8: e60003.
6. Iwasaki Y, Mori K, Ito M, *et al.* An autopsied case of V180I Creutzfeldt-Jakob disease presenting with panencephalopathic-type pathology and a characteristic prion protein type. *Neuropathology* 2011;31:540–8.
7. Yoshida H, Terada S, Ishizu H, *et al.* An autopsy case of Creutzfeldt-Jakob disease with a V180I mutation of the PrP gene and Alzheimer-type pathology. *Neuropathology* 2010;30:159–64.
8. Kono S, Manabe Y, Fujii D, *et al.* Serial diffusion-weighted MRI and SPECT findings in a Creutzfeldt-Jakob disease patient with V180I mutation. *J Neurol Sci* 2011;301:100–3.
9. Jin K, Shiga Y, Shibuya S, *et al.* Clinical features of Creutzfeldt-Jakob disease with V180I mutation. *Neurology* 2004;62:502–5.
10. Kitamoto T, Ohta M, Doh-ura K, *et al.* Novel missense variants of prion protein in Creutzfeldt-Jakob disease or Gerstmann-Straussler syndrome. *Biochem Biophys Res Commun* 1993;191:709–14.
11. Satoh K, Tobiume M, Matsui Y, *et al.* Establishment of a standard 14-3-3 protein assay of cerebrospinal fluid as a diagnostic tool for Creutzfeldt-Jakob disease. *Lab Invest* 2010;90:1637–44.
12. Atarashi R, Satoh K, Sano K, *et al.* Ultrasensitive human prion detection in cerebrospinal fluid by real-time quaking-induced conversion. *Nat Med* 2011;17:175–8.
13. Terasawa Y, Fujita K, Izumi Y, *et al.* Early detection of familial Creutzfeldt-Jakob disease on diffusion-weighted imaging before symptom onset. *J Neurol Sci* 2012;319:130–2.
14. Gambetti P, Kong Q, Zou W, *et al.* Sporadic and familial CJD: classification and characterisation. *Br Med Bull* 2003;66:213–39.
15. Capellari S, Strammiello R, Saverioni D, *et al.* Genetic Creutzfeldt-Jakob disease and fatal familial insomnia: insights into phenotypic variability and disease pathogenesis. *Acta Neuropathol* 2011;121:21–37.
16. Ohkubo T, Sakasegawa Y, Asada T, *et al.* Absence of association between codon 129/219 polymorphisms of the prion protein gene and Alzheimer's disease in Japan. *Ann Neurol* 2003;54:553–4.
17. Chasseigneaux S, Haik S, Laffont-Proust I, *et al.* V180I mutation of the prion protein gene associated with atypical PrPSc glycosylation. *Neurosci Lett* 2006;408:165–9.
18. Xiao X, Yuan J, Haik S, *et al.* Glycoform-selective prion formation in sporadic and familial forms of prion disease. *PLoS ONE* 2013;8: e58786.
19. Parchi P, Castellani R, Capellari S, *et al.* Molecular basis of phenotypic variability in sporadic Creutzfeldt-Jakob disease. *Ann Neurol* 1996;39:767–78.
20. Parchi P, Strammiello R, Giese A, *et al.* Phenotypic variability of sporadic human prion disease and its molecular basis: past, present, and future. *Acta Neuropathol* 2011;121:91–112.
21. Goldfarb LG, Petersen RB, Tabaton M, *et al.* Fatal familial insomnia and familial Creutzfeldt-Jakob disease: disease phenotype determined by a DNA polymorphism. *Science* 1992;258:806–8.
22. Petersen RB, Parchi P, Richardson SL, *et al.* Effect of the D178N mutation and the codon 129 polymorphism on the metabolism of the prion protein. *J Biol Chem* 1996;271:12661–8.
23. Schelzke G, Kretzschmar HA, Zerr I. Clinical aspects of common genetic Creutzfeldt-Jakob disease. *Eur J Epidemiol* 2012;27:147–9.
24. Palmer MS, Dryden AJ, Hughes JT, *et al.* Homozygous prion protein genotype predisposes to sporadic Creutzfeldt-Jakob disease. *Nature* 1991;352:340–2.
25. Petraroli R, Pocchiari M. Codon 219 polymorphism of PRNP in healthy Caucasians and Creutzfeldt-Jakob disease patients. *Am J Hum Genet* 1996;58:888–9.
26. Shibuya S, Higuchi J, Shin RW, *et al.* Codon 219 Lys allele of PRNP is not found in sporadic Creutzfeldt-Jakob disease. *Ann Neurol* 1998;43:826–8.
27. Jeong BH, Lee KH, Kim NH, *et al.* Association of sporadic Creutzfeldt-Jakob disease with homozygous genotypes at PRNP codons 129 and 219 in the Korean population. *Neurogenetics* 2005;6:229–32.
28. Yang TI, Jung DS, Ahn BY, *et al.* Familial Creutzfeldt-Jakob disease with V180I mutation. *J Korean Med Sci* 2010;25:1097–100.
29. Iwasaki Y. Three cases of Creutzfeldt-Jakob disease with prion protein gene codon 180 mutation presenting with pathological laughing and crying. *J Neurol Sci* 2012;319:47–50.
30. Suzuki K, Matsumura N, Suzuki T, *et al.* Creutzfeldt-Jakob disease with V180I mutation and senile plaque. *Geriatr Gerontol Int* 2009;9:210–12.
31. Mutsukura K, Satoh K, Shirabe S, *et al.* Familial Creutzfeldt-Jakob disease with a V180I mutation: comparative analysis with pathological findings and diffusion-weighted images. *Dement Geriatr Cogn Disord* 2009;28:550–7.

BMJ Open

Clinical features of genetic Creutzfeldt-Jakob disease with V180I mutation in the prion protein gene

Temu Qina, Nobuo Sanjo, Masaki Hizume, et al.

BMJ Open 2014 4:
doi: 10.1136/bmjopen-2014-004968

Insights Imaging (2014) 5:375–385
DOI 10.1007/s13244-014-0312-x

PICTORIAL REVIEW

Imaging spectrum of sporadic cerebral amyloid angiopathy: multifaceted features of a single pathological condition

Keita Sakurai · Aya M. Tokumaru · Tomoya Nakatsuka · Shigeo Murayama · Shin Hasebe · Etsuko Imabayashi · Kazutomi Kanemaru · Masaki Takao · Hiroyuki Hatsuta · Kenji Ishii · Yuko Saito · Yuta Shibamoto · Noriyuki Matsukawa · Emiko Chikui · Hitoshi Terada

Received: 14 July 2013 / Revised: 23 December 2013 / Accepted: 13 January 2014 / Published online: 12 February 2014

Abstract
Objectives Sporadic cerebral amyloid angiopathy (CAA) is common cause of cerebrovascular disorders that predominantly affect elderly patients. When symptomatic, cortical-subcortical intracerebral haemorrhage (ICH) in the elderly is the most well-known manifestation of CAA. Furthermore, the clinical presentation varies from a sudden neurological deficit to seizures, transient symptoms and acute progressive cognitive decline. Despite its clinical importance, this multifaceted nature poses a diagnostic challenge for radiologists. The aims of this study were to expound the characteristics of neuroimaging modalities, which cover a wide spectrum of CAA-related imaging findings, and to review the various abnormal findings for which CAA could be responsible.
Conclusions Radiologically, in addition to typical ICH, CAA leads to various types of abnormal findings, including microbleed, subarachnoid haemorrhage, superficial siderosis, microinfarction, reversible oedema, and irreversible leukoaraiosis. Taking into consideration the clinical importance of CAA-related disorders such as haemorrhagic risks and treatable oedema, it is necessary for radiologists to understand the wide spectrum of CAA-related imaging findings.
Teaching Points
- *To describe the characteristics of imaging modalities and findings of CAA-related disorders.*
- *MRI, especially gradient echo sequences, provides the useful information of CAA-related haemosiderin depositions.*
- *To understand the wide spectrum of CAA-related neuroimaging and clinical features is important.*

Keywords Cerebral amyloid angiopathy · Imaging · Subarachnoid haemorrhage · Microbleed · Superficial siderosis · CAA-related inflammation

K. Sakurai (✉) · A. M. Tokumaru · S. Hasebe · E. Imabayashi
Department of Diagnostic Radiology, Tokyo Metropolitan Medical Centre of Gerontology, 35-2 Sakaecho, Itabashi-ku, Tokyo 173-0015, Japan
e-mail: ksak666@yahoo.co.jp

T. Nakatsuka · H. Terada
Department of Radiology, Toho University Sakura Medical Centre, Sakura, Japan

S. Murayama · M. Takao · H. Hatsuta
Department of Neuropathology (the Brain Bank for Aging Research), Tokyo Metropolitan Geriatric Hospital, Tokyo Metropolitan Geriatric Hospital and Institute of Gerontology, Tokyo, Japan

K. Kanemaru
Department of Neurology, Tokyo Metropolitan Geriatric Hospital, Tokyo, Japan

K. Ishii
Positron Medical Centre, Tokyo Metropolitan Institute of Gerontology, Tokyo, Japan

Y. Saito
Department of Pathology and Laboratory Medicine, National Centre for Neurology and Psychiatry Hospital, Tokyo, Japan

Y. Shibamoto
Department of Radiology, Nagoya City University Graduate School of Medical Sciences, Nagoya, Japan

N. Matsukawa
Department of Neurology and Neuroscience, Nagoya City University Graduate School of Medical Sciences, Nagoya, Japan

E. Chikui
Department of Neurosurgery, Tokyo Metropolitan Geriatric Hospital, Tokyo, Japan

Introduction

Sporadic cerebral amyloid angiopathy (CAA) is a common small vessel disease of the brain, characterised by the progressive deposition of amyloid-β (Aβ) protein in the walls of small- to medium-sized arteries (up to about 2 mm in diameter), arterioles and capillaries in the cerebral cortex and overlying leptomeninges, preferentially affecting occipital regions for unclear reasons. In contrast to the amyloid plaques found in Alzheimer disease (AD), which are predominantly composed of the 42-amino-acid-residue fragment, the vascular amyloid in CAA is mostly composed of the more soluble, 40-amino-acid fragment, which suggests different pathophysiological mechanisms for pathological deposition [1]. Impairment in one or more elimination mechanisms may result in the accumulation of Aβ in the walls of small- and medium-sized leptomeningeal and cortical blood vessels. Upon autopsy, CAA may be found more commonly in women than in men. The incidence of CAA, like AD, is strongly age-dependent. Although found at autopsy in only 33 % of 60–70 year olds, the prevalence of age-related CAA increases to 75 % among those older than 90 years [2]. Despite its high prevalence, CAA remains an underestimated cause of cerebrovascular disease, both clinically and at imaging, in part because many patients are asymptomatic. When symptomatic, intracerebral haemorrhage (ICH) in the elderly is the most well-known manifestation. Furthermore, the clinical presentation varies from a sudden neurological deficit to seizures, transient symptoms and cognitive decline, including acute progressive dementia. However, these symptoms are not specific and are often not readily associated with CAA.

Radiologically, in addition to typical acute cortical-subcortical ICH, CAA leads to various types of abnormal findings, including chronic ICHs, microbleed (MB), subarachnoid haemorrhage (SAH), superficial siderosis (SS), microinfarction, reversible oedema and irreversible leukoaraiosis (Table 1) [3]. Taking into consideration the clinical importance of CAA-related haemorrhagic risks in the setting of antiplatelet, anticoagulation and thrombolysis therapies, as well as treatable oedema [3–6], it is necessary for radiologists to understand the wide spectrum of CAA-related imaging findings.

The aims of this study were the following: to expound the characteristics of neuroimaging modalities, including computed tomography (CT), magnetic resonance imaging (MRI) and positron emission tomography (PET), which cover a wide spectrum of CAA-related imaging findings, and to review the various abnormal findings for which CAA could be responsible. The recognition of wide-spectrum imaging findings can be useful for radiologists not only to raise the possibility of CAA but also to precisely comprehend the pathophysiology of CAA and management to improve the prognosis.

Neuroimaging modalities: critical roles in the diagnosis of CAA

CT

CT is the initial screening modality for patients with various symptoms, especially acute neurological deficits or transient ischaemic attack-like symptoms, which can allow rapid establishment of the presence or absence of ICHs and SAHs. CT can provide crucial information regarding the characteristics of these haemorrhagic conditions, including volume, shape and distribution. Additional CT angiography with intravenous contrast media is useful to exclude other pathological conditions (e.g. aneurysms, arteriovenous malformation, fistula and venous thrombosis) that could cause similar haemorrhagic complications.

On CT scan, cortical-subcortical ICHs without a history of hypertension and sulcal SAHs without a history of head trauma can be the findings suggestive of CAA. However, it is difficult to evaluate other findings, such as MBs and SS, which support the diagnosis of CAA. The disadvantage of CT is lower contrast resolution than MRI, which can depict acute cerebral infarctions, MBs and white matter lesions more clearly. In other words, CAA cannot be diagnosed by CT alone, but requires MRI sequences sensitive to susceptibility effects.

MRI

The important point of MRI in the diagnosis of CAA is to perform the proper sequences to cover a wide spectrum of CAA-related abnormal findings including not only haemorrhages but also oedemas and infarctions. Therefore, the standard imaging protocol should include at least the gradient-echo (GRE), fluid-attenuated inversion recovery (FLAIR) and diffusion-weighted imaging (DWI). The standard MRI protocol is shown in Table 2.

The optimal detection of haemorrhagic lesions, including MB and SS, depends on multiple MRI parameters, including pulse sequence, spatial resolution, echo time and field strength. Due to CAA-related pathological changes such as haemosiderin accumulations which lead to large variations in local magnetic fields and a local reduction in T2*, it is necessary to perform the GRE sequence, which is more sensitive to the magnetic susceptibility effect than turbo spin-echo sequences, in the diagnosis of CAA [7]. In the elderly, GRE sequences are essential to check for CAA-related MBs and/or SAH, which can potentially predict life-threatening lobar haemorrhages [8]. Compared with conventional 2D sequences, increasing spatial resolution (i.e. smaller voxel size) on 3D sequence improves the detection of MBs [9]. A longer echo time enables more efficient detection of MBs than a shorter one due to the blooming effect [9]. In addition to these parameters, higher susceptibility effects and increase of

Table 1 CAA-related abnormal imaging findings

Disease	Imaging findings	Recommended neuroimaging modality
ICH	Haematoma with distinctive cortical-subcortical distribution generally sparing the deep white matter and basal ganglia and brainstem	CT and MRI **MRI**; additional depiction of chronic haemosiderin depositions and MBs
MBs	Small round hypointense foci on MRI	MRI, especially susceptibility-weighted image
SAH	Supratentorial sulcal high attenuation/intensity, most frequently depicted around the precentral gyrus	CT and MRI **MRI**; additional depiction of MB and SS
SS	Hypointensity along the supratentorial cerebral sulcus on MRI	MRI, especially susceptibility-weighted image
CAA-related inflammation	Large confluent asymmetric abnormal attenuation/intensity mainly in the subcortical WM	CT and MRI **MRI**; additional evaluation of vasogenic oedema and other findings such as MB and SS
Leukoaraiosis	Low attenuation on CT and high intensity on FLAIR and T2W MRI mainly in the deep WM with sparing of the subcortical U fibres	CT and MRI MRI; depiction of leukoaraiosis clearer than CT
Microinfarction	Small ovoid or round high intensity of the subcortical and cortex on diffusion-weighted image	MRI, especially diffusion-weighted image

CAA cerebral amyloid angiopathy, *CT* computed tomography, *FLAIR* fluid-attenuated inversion recovery, *ICH* intracerebral haemorrhage, *MRI* magnetic resonance imaging, *MB* microbleed, *SAH* subarachnoid haemorrhage, *SS* superficial siderosis, *T2W* T2-weighted, *WM* white matter

signal-to-noise ratio with field strength improve the detection of MBs at a 3-T imager compared with a 1.5-T one [9]. Taking these parameters into consideration, it is reasonable to perform sophisticated 3D sequences with higher spatial resolution and longer echo time including a susceptibility-weighted image (SWI) and the principles of echo-shifting with a train of observations (PRESTO) image to detect MB and SS [9, 10]. Notably, SWI with smaller section thickness and higher magnetic field is currently the most sensitive technique to visualise MBs, which combines both magnitude information and phase information to accentuate the visibility of susceptible foci. These sequences can be of potential value in the evaluation of CAA patients (Fig. 1).

However, the GRE sequence is less sensitive than the FLAIR sequence for the detection of acute SAHs and parenchymal changes. The better lesion/tissue contrast achieved by the suppression of the signal intensity of cerebrospinal fluid (CSF) on the FLAIR sequence not only in the subarachnoid space, but also in the cerebral parenchyma can be especially useful for the evaluation of CAA-related white matter lesions and SAHs. In addition to these sequences, DWI with apparent diffusion coefficient (ADC) maps can be useful to distinguish CAA-related silent infarctions from other white matter lesions, including vasogenic oedema and leukoaraiosis [3, 5].

PET

Although clinical criteria based on MRI and CT findings have been validated for a pre-mortem diagnosis of CAA during life [11], this relies on detecting late manifestations of CAA-related vascular damage such as ICHs and MBs rather than the vascular amyloid itself. Therefore, these morphological

Table 2 Standard MRI protocol for the diagnosis of CAA

Sequence	Expected role for the diagnosis
Minimum required protocol	
T2*-weighted image	Depiction of haemosiderin depositions suggestive of chronic ICHs, MBs and SS
Fluid-attenuated inversion recovery image	Depiction of acute and subacute SAHs, and white matter signal changes
Diffusion-weighted image	Depiction of acute microinfarction Evaluation of vasogenic oedema due to CAA-related inflammation
Optional sequence for the diagnosis of CAA	
Susceptibility-weighted image	Depiction of haemosiderin depositions, clearer than T2*-weighted image
Additional sequences for differential diagnosis	
T1-weighted image	Depiction of T1 shortening due to methaemoglobin and melanin
Contrast-enhanced T1-weighted image	Differentiation between haemorrhagic tumours and other lesions
Magnetic resonance angiogram	Evaluation of vascular disorders such as vasculitis

CAA cerebral amyloid angiopathy, *ICH* intracerebral haemorrhage, *MB* microbleed, *MRI* magnetic resonance imaging, *SAH* subarachnoid haemorrhage, *SS* superficial siderosis

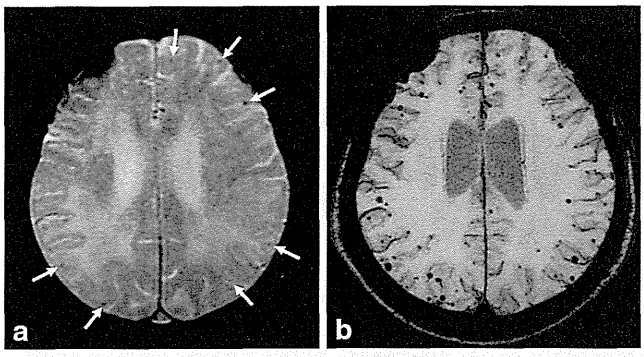

Fig. 1 Multiple MBs and CAA-related inflammation in a 78-year-old man. In addition to the right dominant diffuse white matter lesions, an axial GRE T2*-weighted image on the 1.5-T imager (**a**) revealed some cortical-subcortical hypointense foci suggestive of CAA-related MBs (*arrows*). Of note, more hypointense foci in the posterior dominant distribution were identified on the corresponding PRESTO image (**b**)

techniques cannot lead to a correct diagnosis in a definite proportion of CAA patients during life. However, an emerging functional technique, Pittsburgh compound B (PiB) PET imaging to measure the burden and location of fibrillar Aβ deposits, has recently been reported as a promising technique for CAA detection [12]. In addition to binding to fibrillar senile plaques, this radiotracer can clearly delineate the vascular amyloid before it triggers haemorrhagic complications or other overt small-vessel brain injuries, and can be a useful clue to diagnose not only AD but also CAA [13].

In the case of coexisting CAA and hypertension, the widespread involvement of arterioles by both types of arteriopathy likely causes the progression of small vessel disease and some overlap in the distribution of MBs [14]. In such cases, PiB-PET can provide a definite clue not only for the diagnosis of CAA but also the coexistence of hypertensive arteriopathy (Fig. 2). However, it is important to understand that PIB is a non-specific imaging marker of Aβ peptide-related cerebral amyloidosis. As previously mentioned, this tracer labels vascular as well as plaque Aβ; therefore, differentiating PiB signal caused by CAA from that caused by other kinds of plaques is difficult.

Representative imaging findings: multifaceted features of a single pathological condition

Lobar haemorrhage: a life-threatening sign

CAA is one of the most common causes of lobar ICHs in the elderly [15]. In addition to the advanced age, hypertension and minor head injuries may increase the risk of CAA-related ICHs [15, 16]. The clinical presentation of CAA-related ICH varies according to ICH size and location. Patients commonly present with an acute stroke syndrome with focal neurological deficits that may be associated with headache, vomiting, seizures and/or an altered level of consciousness. In the longer term, survivors of lobar ICHs are at a high risk of recurrence, especially with the presence of the ε2 or ε4 alleles of the apolipoprotein E gene (28 % cumulative recurrence rate at 2 years relative to 10 % in patients without either allele) [17].

Regardless of the size, CAA-related ICHs exhibit distinctive cortical-subcortical distributions that generally spare the deep white matter, basal ganglia and brainstem. This cortical-subcortical distribution of CAA-related ICHs has been correlated with the anatomical distribution of β-amyloid-containing vessels. Notably, haemorrhagic lesions are shown to be preferentially distributed in the temporal and occipital lobes, and are likely to cluster regardless of the lobes [18]. Comprehension of this characteristic distribution was validated by the Boston criteria, which are most commonly used and highly specific for the diagnosis of CAA (Table 3) [11, 19]. CAA-related macrohaemorrhages may be associated with subarachnoid, subdural or, less commonly, intraventricular haemorrhage (Figs. 3 and 4) [8]. Other neuroimaging findings suspicious for CAA-related ICHs include the multiplicity and recurrence of ICHs (Fig. 4). Recurrent haemorrhages are typically lobar, often in the same lobe as the initial CAA-related ICHs [18]. CT is sufficient to provide crucial information regarding the characteristics of acute CAA-related ICHs. However, MRI examinations including GRE sequences should be performed to evaluate chronic haemosiderin depositions and MBs, which can be useful to diagnose CAA.

Microbleeds: easily overlooked but a suggestive sign of CAA

This finding indicates previous extravasation of blood-related to bleeding-prone microangiopathy, including CAA and hypertensive arteriopathy (Fig. 5) [14]. In the pathological analysis of lobar MBs in CAA patients, various CAA-related pathologies, including acute microhaemorrhages, haemosiderin residua of old haemorrhages and small lacunes ringed by haemosiderin, are proved to produce signal voids on SWI [20]. MBs located in lobar regions may correlate with disease progression, recurrent ICH, and cognitive dysfunctions [21, 22]. Moreover, early recognition can be advantageous to patients on antiplatelet or thrombolysis therapy in that they are at an increased risk for subsequent and possibly fatal haemorrhages [4, 6].

MBs are typically defined on GRE sequences as small, well-demarcated, hypointense, rounded foci less than 5–10 mm in size, which are distinct from cortical vascular flow voids, leptomeningeal siderosis, or non-haemorrhagic subcortical mineralisation such as symmetrical hypointensities in the globus pallidus [21]. The presence of multiple, strictly lobar, cortical-subcortical MBs detected by GRE sequences has been shown to be highly specific for severe CAA in elderly patients with no other definite cause of ICH, such as trauma, ischaemic stroke, coagulopathy or excessive anticoagulation (probable